EAI Endorsed Transactions
on Scalable Information Systems
Research Article EAI.EU

Real-Time Task Fault-Tolerant Scheduling Algorithm for Dynamic Monitoring Platform of Distribution Network Operation under Overload of Distribution Transformer

Hancong Huangfu[1,*], Yongcai Wang[1], and Jiang Jiang[2]

[1]Foshan Power Supply Bureau of Guangdong Power Grid Co., Ltd., Foshan 528000, Guangdong, China.
[2]Guangdong Power Grid, Guangzhou Guangdong 510000,China.

Abstract

This paper proposes a real-time task fault-tolerant scheduling algorithm for a dynamic monitoring platform of distribution network operation under overload of distribution transformers. The proposed algorithm is based on wireless communication and mobile edge computing to address the challenges faced by distribution networks in handling the increasing load demand. For the considered system, we evaluate the system performance by analyzing the communication and computing latency, from which we then derive an analytical expression of system outage probability to facilitate the performance evaluation. We further optimize the system design by allocating computing resources for multiple mobile users, where a greedy-based optimization scheme is proposed. The proposed algorithm is evaluated through simulations, and the results demonstrate its effectiveness in reducing task completion time, improving resource utilization, and enhancing system reliability. The findings of this study can provide a basis for the development of practical solutions for the dynamic monitoring of distribution networks.

Received on 19 March 2023; accepted on 30 April 2023; published on 11 May 2023

Keywords: Edge computing, wireless communication, task scheduling, dynamic monitoring.

doi:10.4108/eetsis.v10i3.3158

1. Introduction

Motivated by the development of wireless communication and edge computing [1–4], real-time task fault-tolerant scheduling (RTTFTS) is an important problem in real-time systems, which aims to provide timely execution of tasks even in the presence of failures [5–7]. In recent years, several studies have focused on developing efficient RTTFTS algorithms that can handle different types of faults, such as processor failures, memory failures, and communication failures. One of the early studies in RTTFTS was a fault-tolerant scheduling algorithm based on redundancy, where the algorithm duplicated each task and assigned them to different processors to ensure fault-tolerance. However, this approach suffers from high redundancy overheads and may not be scalable for large systems. In a more recent study, an RTTFTS algorithm was proposed based on mixed-criticality scheduling (MCS), which can assign different levels of criticality to tasks based on their importance, and schedule them accordingly. It took advantage of MCS to provide fault-tolerance by assigning backup tasks to low criticality tasks. The results showed that this algorithm could achieve a better fault-tolerance than traditional approaches. Another recent study was the RTTFTS algorithm that considered both task-level and system-level fault-tolerance, where the tasks were scheduled based on the deadlines and priorities, while also considered the availability of redundant resources. This algorithm was evaluated using simulations and showed significant improvement in fault-tolerance compared to traditional approaches. In a different approach, an RTTFTS algorithm was proposed

*Corresponding author. Email: HancongHuangfu@126.com, huangfuhancong@gdfs.csg.cn.

based on dynamic partial order reduction (DPOR), which could reduce the search space of scheduling algorithms by eliminating redundant schedules. This algorithm used DPOR to efficiently handle faults and reduced the computational overhead of scheduling. The results showed that this algorithm could handle more faults than traditional approaches, while also reducing the scheduling overhead.

Wireless communication [8–10] and edge computing [11–13] are two key technologies that are increasingly being used in dynamic monitoring platforms. These platforms are designed to collect, process, and analyze data from a wide range of sensors and devices in real-time, in order to provide insights and support decision-making across a variety of industries and applications [14–16]. One recent study examined the use of a dynamic monitoring platform for agricultural applications. This platform consisted of wireless sensor nodes deployed throughout a vineyard, which collected data on temperature, humidity, and soil moisture. The data was then processed using edge computing techniques, and the resulting insights were used to optimize irrigation and fertilizer use. Another study looked at a dynamic monitoring platform for traffic management. The platform used a combination of wireless sensors and edge computing to collect data on traffic flow, speed, and congestion, and to provide real-time feedback to drivers and traffic management systems. It could be that the platform was effective in reducing traffic congestion and improving overall traffic flow. In the field of healthcare, dynamic monitoring platforms are also being developed to support remote patient monitoring and personalized medicine. One recent study described the use of a wireless, wearable device for monitoring glucose levels in diabetic patients. The device collected data in real-time and used edge computing techniques to provide personalized feedback and recommendations to patients based on their individual glucose profiles.

This paper presents a novel real-time task fault-tolerant scheduling algorithm designed for a dynamic monitoring platform of distribution network operation, which is frequently subjected to overload from distribution transformers. The proposed algorithm utilizes wireless communication and mobile edge computing to overcome the challenges associated with the increasing load demand. For the considered system, we evaluate the system performance by analyzing the communication and computing latency, from which we then derive an analytical expression of system outage probability to facilitate the performance evaluation. We further optimize the system design by allocating computing resources for multiple mobile users, where a greedy-based optimization scheme is proposed. Through simulations, the effectiveness of the proposed algorithm in reducing task completion time, improving resource utilization, and enhancing system reliability is demonstrated. The findings of this study offer a practical solution for the dynamic monitoring of distribution networks.

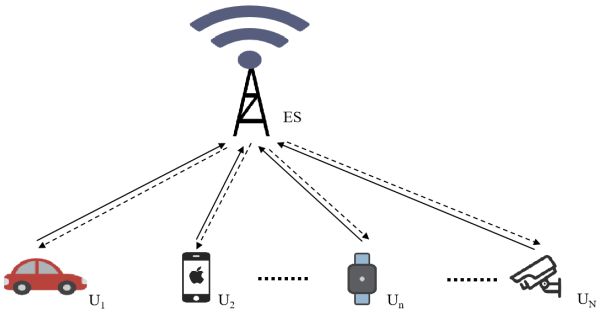

Figure 1. System model of multi-user MEC for dynamic monitoring.

2. System Model

Fig. 1 depicts the system model of the multi-user MEC network for dynamic monitoring, where N mobile users have some latency sensitive computational tasks and need to be offloaded to one edge server. Specifically, $\mathcal{U} \triangleq \{U_1, U_2, \ldots, U_N\}$ is the N mobile users set, where mobile user U_n has one task with the task size of L that needs to be offloaded and computed at the edge server. Due to requirement on the latency sensitive tasks, all tasks from N mobile users need to be finished under a given latency threshold γ_t. In the following, we will detail the system latency of considered MEC system.

In the MEC system, mobile user U_n needs to offload its task to the edge server. According to the Shannon theorem, the data transmission rate of mobile user U_n can be given by [17–19]

$$R_n = B \log_2 \left(1 + \frac{p|h_n|^2}{\sigma^2}\right), \tag{1}$$

where the channel parameter of the link between mobile user U_n and the edge server is represented by h_m, while the wireless bandwidth between them is denoted as B. The transmit power of the mobile user is represented by p, and σ^2 is the variance of additive white Gaussian noise (AWGN) [20–23]. From (1), we can further give the transmission latency of mobile user U_n as [24, 25]

$$T_n^{\text{trans}} = \frac{L}{R_n}. \tag{2}$$

The edge server receives the tasks offloaded from mobile users and then will compute the task. Assume that the computational resource at the edge server can be allocated to different tasks from all users, thus all the received tasks can be computed in parallel. The

corresponding computation latency of mobile user U_n's task can be given by

$$T_n^{\text{comp}} = \frac{\omega L}{f_n}, \tag{3}$$

where f_n is the computational resource allocated to mobile user U_n's task, which satisfies $\sum_{n=1}^{N} \leq f_{total}$, in which f_{total} is the total computational resource at the edge server, and ω is the needed CPU cycle to compute one bit of computational task.

Thus, the total task offloading latency of mobile user U_n can be given by [26, 27]

$$T_n^{\text{total}} = T_n^{\text{trans}} + T_n^{\text{comp}}. \tag{4}$$

3. Outage Probability

In this section, we analyze the outage performance for the considered MEC system. By defining the user outage and system outage, we are able to analyze system performance under a given latency threshold. Specifically, the outage event of mobile user U_n can be defined as its total task offloading latency exceeds the latency threshold γ_t. Therefore, the corresponding outage probability can be given by

$$P_n^{\text{out}} = \Pr[T_n^{\text{total}} \geq \gamma_t]. \tag{5}$$

From (5), we can further define the system outage probability as

$$P^{\text{out}} = \frac{1}{N}\sum_{n=1}^{N} \Pr[T_n^{\text{total}} \geq \gamma_t]. \tag{6}$$

In the following, we will derive a closed-form outage probability for both users and the considered MEC system. Specifically, we can rewrite (5) as [28, 29]

$$P_n^{\text{out}} = \Pr[T_n^{\text{trans}} + T_n^{\text{comp}} \geq \gamma_t], \tag{7}$$

$$= 1 - \Pr[T_n^{\text{trans}} + T_n^{\text{comp}} \leq \gamma_t], \tag{8}$$

$$= 1 - \Pr\left[\frac{L}{B\log_2\left(1+\frac{p|h_n|^2}{\sigma^2}\right)} + \frac{\omega L}{f_n} \leq \gamma_t\right], \tag{9}$$

$$= 1 - \Pr\left[\frac{L}{B\log_2\left(1+\frac{p|h_n|^2}{\sigma^2}\right)} \leq \gamma_t - \frac{\omega L}{f_n}\right]. \tag{10}$$

After some manipulations, we can further have,

$$P_n^{\text{out}} = 1 - \Pr\left[|h_n|^2 \geq \frac{2^{\frac{L}{B\left(\gamma_{th}-\frac{\omega L}{f_n}\right)}}-1}{\frac{p}{\sigma^2}}\right], \tag{11}$$

$$= \Pr\left[|h_n|^2 \leq \frac{2^{\frac{L}{B\left(\gamma_{th}-\frac{\omega L}{f_n}\right)}}-1}{\frac{p}{\sigma^2}}\right]. \tag{12}$$

Note that mobile user U_n experiences Rayleigh flat fading in the offloading, with an average channel gain of λ_n, and we further have

$$P_n^{\text{out}} = 1 - \exp\left(\frac{1-\exp\left(\frac{L\ln 2}{B\left(\gamma_{th}-\frac{\omega L}{f_n}\right)}\right)}{\frac{\lambda_n p}{\sigma^2}}\right), \tag{13}$$

$$= 1 - \exp\left(\frac{1-\exp\left(\frac{L\ln 2}{B\left(\gamma_{th}-\frac{\omega L}{f_n}\right)}\right)}{\frac{\lambda_n p}{\sigma^2}}\right). \tag{14}$$

Then, substituting (14) into (6), we can obtain the MEC system outage probability as

$$P^{\text{out}} = \frac{1}{N}\sum_{n=1}^{N} \Pr[T_n^{\text{total}} \geq \gamma_t], \tag{15}$$

$$= \frac{1}{N}\sum_{n=1}^{N}\left(1 - \exp\left(\frac{1-\exp\left(\frac{L\ln 2}{B\left(\gamma_{th}-\frac{\omega L}{f_n}\right)}\right)}{\frac{\lambda_n p}{\sigma^2}}\right)\right). \tag{16}$$

In order to obtain more insight on the considered MEC system, we use (16) to derive an asymptotic expression of P^{out} in high SNR case, which can be given by

$$P^{\text{out}} = \frac{1}{N}\sum_{n=1}^{N}\left(1 - \exp\left(\frac{1-\exp\left(\frac{L\ln 2}{B\left(\gamma_{th}-\frac{\omega L}{f_n}\right)}\right)}{\frac{\lambda_n p}{\sigma^2}}\right)\right), \tag{17}$$

$$\simeq \frac{1}{N}\sum_{n=1}^{N}\left(1 - \left(1 - \frac{\exp\left(\frac{L\ln 2}{B\left(\gamma_{th}-\frac{\omega L}{f_n}\right)}\right)-1}{\frac{\lambda_n p}{\sigma^2}}\right)\right), \tag{18}$$

$$= \frac{1}{N}\sum_{n=1}^{N}\left(\frac{\exp\left(\frac{L\ln 2}{B\left(\gamma_{th}-\frac{\omega L}{f_n}\right)}\right)-1}{\frac{\lambda_n p}{\sigma^2}}\right), \tag{19}$$

$$= P_{\text{out}}^{\text{asym}}, \tag{20}$$

where $\lim_{w\to 0} e^{-w} \simeq 1 - w$ is used.

With the asymptotic outage probability $P_{\text{out}}^{\text{asym}}$, several insights on the MEC system can be obtained. Specifically, the system outage improves with an increase in B, p, and λ_n, indicating that higher transmission rates can enhance the system performance. Moreover, the system outage deteriorates with a larger task size L, indicating a larger tasks size will increase both the latency of task transmission and computation. In further, the computational resource f_n affect the system outage, since a

larger allocated computational resource will cause less computation latency.

According the above insights, we can find that it is of vital importance to allocate the computational resource. Thus, in the next section, we will propose a greedy based method to solve the computational resource allocation problem.

4. Greedy based computational resource allocation

In this section, we use a greedy based method to allocate the total computational resource. We optimize $\{f_1, \ldots, f_N\}$ to minimize the system outage.

First, we relax the total computational resource constraint and assume that all mobile users can be assigned with sufficient computational resource to finish the computation within the latency threshold γ_t, given by

$$\frac{L}{B\log_2\left(1+\frac{p|h_n|^2}{\sigma^2}\right)}+\frac{\omega L}{f_n^{need}}=\gamma_t, \tag{21}$$

where f_n^{need} is the required computational resource.

Then, we can calculate the required computational resource f_n^{need} as,

$$f_n^{need}=\frac{\omega L}{\left(\gamma_t-\frac{L}{B\log_2\left(1+\frac{p|h_n|^2}{\sigma^2}\right)}\right)}. \tag{22}$$

If the total required computational resource $\sum_{n=1}^{N} f_n^{need}$ exceeds f_{total}, we will drop the mobile users in descending order of f_n^{need}, and assign no computational resource to them until the computational resource constraint $\sum_{n=1}^{N} \leq f_{total}$ is met.

5. Simulation

In this section, we provide some simulations to to validate the proposed studies. If not specified, "Simulation", "Analysis", and "Asymptotic" are performed with equally allocated bandwidth and computational resource, and "Greedy" is the simulated outage with the greedy based computational resource allocation. Besides, we set the mobile user number $N = 5$, and set the task size $L = 50$Mbits. Moreover, each mobile user's transmit power p is 1W and σ^2 is 0.001. In further, the total bandwidth is 30MHz, and it is equally allocated to each mobile user. The total computational resource at edge server is 5 GHz, and $\omega = 10$. For the Rayleigh flat fading channels, the average channel gain of each user is uniformly distributed as $\lambda_n \in \mathcal{U}(0.5, 1.5)$.

Figure 2 and Table 1 depict the system outage probability versus the transmit SNR for $N = 3$ and $N = 5$, where the transmit SNR ranges from 0 dB to 40 dB. This figure and table show that both the analytical

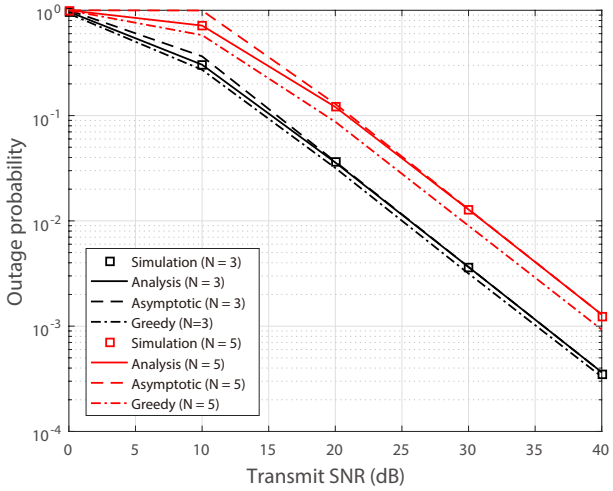

Figure 2. System outage probability versus SNR.

Table 1 Numerical P_{out} versus SNR

SNR/db	0	10	20	30	40
Sim. N=3	0.9673	0.3037	0.0358	0.0036	3.506e-4
Ana. N=3	0.9673	0.3037	0.0358	0.0036	3.506e-4
Asy. N=3	1	0.3652	0.0365	0.0037	3.512e-4
Greedy N=3	0.9275	0.2722	0.0318	0.0031	3.311e-4
Sim. N=5	0.9999	0.7161	0.1206	0.0128	0.0012
Ana. N=5	0.9999	0.7161	0.1206	0.0128	0.0012
Asy. N=5	1	0.9951	0.1291	0.0129	0.0013
Greedy N=5	0.9980	0.5807	0.0872	0.0089	9.280e-4

results and simulation data for outage probability have the same slope for both $N = 3$ and $N = 5$ cases. Additionally, the asymptotic system outage probability closely follows the analytical curve when the transmit SNR is large, and the accuracy of the derived analytical and asymptotic P_{out} is demonstrated. Moreover, the results show that all metrics improve as the transmit SNR increases, indicating that a higher transmit power can enhance the task offloading. In further, the outage performance is better for $N = 3$ than that for $N = 5$, as fewer resources are allocated per user when there are more mobile users, leading to an increased competition among users. Furthermore, the proposed greedy based method outperforms the uniform allocation, showing its ability in utilizing the computational resource.

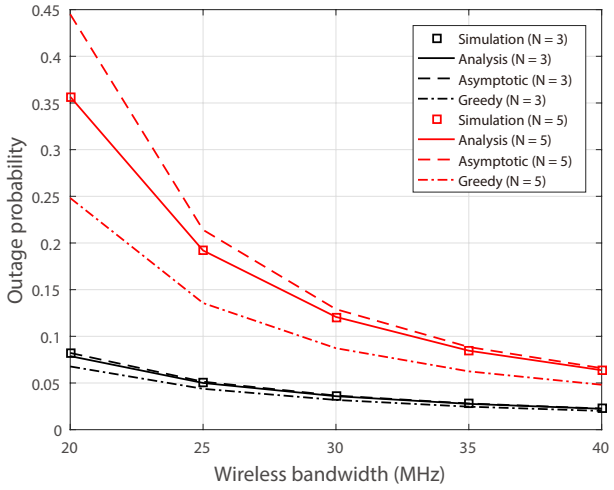

Figure 3. P_{out} versus the bandwidth B.

Table 2 Numerical P_{out} versus B.

B_{total}/MHz	20	25	30	35	40
Sim. N=3	0.0822	0.0498	0.0358	0.0276	0.0224
Ana. N=3	0.0822	0.0498	0.0358	0.0276	0.0224
Asy. N=3	0.0822	0.0513	0.0365	0.0280	0.0226
Greedy N=3	0.0677	0.0437	0.0318	0.0246	0.0201
Sim. N=5	0.3568	0.1917	0.1206	0.0844	0.0638
Ana. N=5	0.3568	0.1917	0.1206	0.0844	0.0638
Asy. N=5	0.4450	0.2140	0.1290	0.0885	0.0659
Greedy N=5	0.2481	0.1356	0.0872	0.0624	0.0481

In Fig. 3 and Table 2, the outage probability of the system is shown against the wireless bandwidth, with $N = 3$ and $N = 5$ mobile users. The total wireless bandwidth ranges from 20 MHz to 40 MHz. This figure and table indicate that the simulation, as well as the analytical and asymptotic approaches, have the same slope for both $N = 3$ and $N = 5$ cases. This confirms the accuracy of the analytical and asymptotic methods for calculating the system outage probability. Moreover, a larger wireless bandwidth enhances the system's outage performance, indicating that a wider wireless bandwidth can improve the transmission of the task. It is also evident that the case with $N = 3$ users performs better than the case with $N = 5$ users because a smaller number of users can improve task offloading. Furthermore, the proposed greedy-based method outperforms the uniform allocation, demonstrating its ability to allocate computational resources effectively.

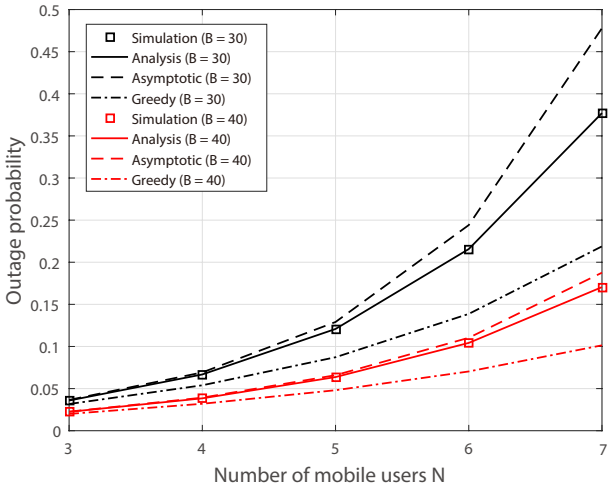

Figure 4. System outage probability versus the number of mobile user N.

Table 3 Data for Fig.4

N	3	4	5	6	7
Sim. B_{total}=30MHz	0.0359	0.0668	0.1208	0.2155	0.3772
Ana. B_{total}=30MHz	0.0359	0.0668	0.1208	0.2155	0.3772
Asy. B_{total}=30MHz	0.0365	0.0692	0.1290	0.2441	0.4779
Greedy B_{total}=30MHz	0.0317	0.0539	0.0872	0.1386	0.2188
Sim. B_{total}=40MHz	0.0224	0.0383	0.0635	0.1039	0.1701
Ana. B_{total}=40MHz	0.0224	0.0383	0.0635	0.1039	0.1701
Asy. B_{total}=40MHz	0.0226	0.0392	0.0659	0.1103	0.1876
Greedy B_{total}=40MHz	0.0199	0.0319	0.0480	0.0703	0.1013

Figure 4 and Table 3 illustrate how the system outage probability is affected by the number of mobile users for wireless bandwidths of 30MHz and 40MHz, with the number of users ranging from 3 to 7. As shown in the figure and table, the analytical and asymptotic outage probability values derived for both bandwidth cases converge well with simulation results, validating their accuracy. Additionally, as the number of mobile users increases, the system outage performance deteriorates due to increased resource competition

among users. Moreover, the curves with a larger bandwidth outperform those with a smaller value, indicating that a larger bandwidth improves offloading performance. In further, the proposed greedy-based method is more effective than uniform allocation in allocating computational resources, demonstrating its ability to optimize resource allocation.

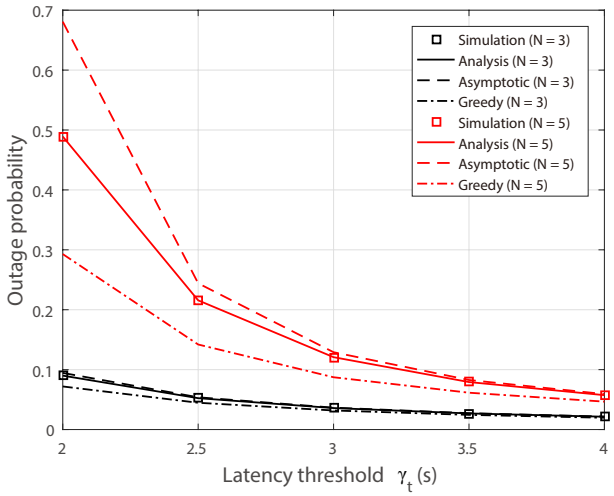

Figure 5. System outage probability versus the latency threshold γ_t.

Table 4 Data for Fig.5

γ_t/s	2	2.5	3	3.5	4
Sim. N=3	0.0898	0.0524	0.0358	0.0268	0.0213
Ana. N=3	0.0898	0.0524	0.0358	0.0268	0.0213
Asy. N=3	0.0944	0.0538	0.0365	0.0272	0.0216
Greedy N=3	0.0719	0.0447	0.0318	0.0244	0.0196
Sim. N=5	0.4889	0.2155	0.1206	0.0793	0.0573
Ana. N=5	0.4889	0.2155	0.1206	0.0793	0.0573
Asy. N=5	0.6808	0.2441	0.1290	0.0827	0.0591
Greedy N=5	0.2928	0.1419	0.0872	0.0614	0.0465

In Fig. 5 and Table 4, we observe the impact of latency threshold on the system outage probability for two values of the number of mobile users, $N = 3$ and $N = 5$, with the latency threshold ranging from 2s to 4s. The figure and table show that the derived analytical and asymptotic outage probabilities converge well with simulation, thereby validating the accuracy of the analytical and asymptotic system outage probability. Moreover, the figure shows that an increase in the latency threshold results in a decrease in the system outage probability, suggesting that having more time to offload tasks can decrease the system outage. Additionally, the curves corresponding to a smaller N perform better than those corresponding to a larger N, implying that reducing the number of mobile users can improve offloading performance. In further, the proposed greedy-based method for allocating computational resources is more effective than uniform allocation, as shown in our simulations. This demonstrates the ability of the method to optimize resource allocation.

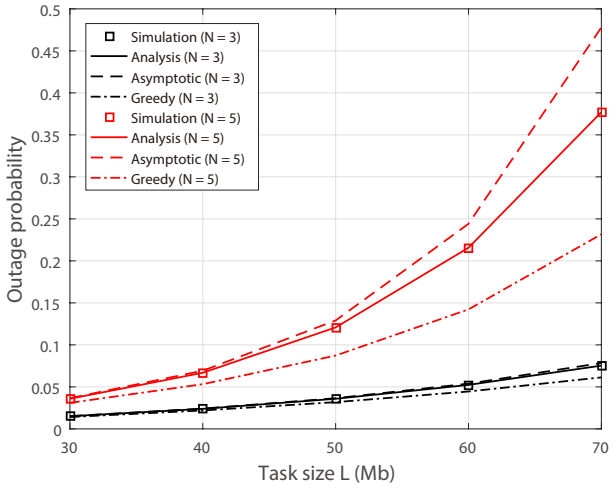

Figure 6. System outage probability versus the task size L.

Fig. 6 and Table 5 show the outage probability of the system versus the task size L, where the task size L varies from 30Mb to 70Mb and the number of mobile users is 3 and 5, respectively. Observations can be made from both the figure and table, indicating that the analysis and the asymptotic have similar results to the simulation for both $N = 3$ and $N = 5$ when the task size varies, which proves the correctness of the derived expressions in computing P_{out}. Moreover, the outage probabilities increase as the task size increases, since a larger task requires more communication resources deteriorating the communication of the system. In further, the outage probabilities with $N = 5$ are higher than that with $N = 3$, as more mobile devices cause more intense resource competition which increases the system outage probability.

Fig. 7 and table 6 show the impact of the computational resource on the system outage probability, where the computational resource varies from 1GHz to 9GHz and the number of mobile users is 3 and 5, respectively. From Fig. 7 and table 6, we can see that the analysis and the asymptotic have similar results to the simulation for both $N = 3$ and $N = 5$ when the computational resource

Table 5 Data for Fig.6

L/Mbit	30	40	50	60	70
Sim. N=3	0.0148	0.0237	0.0358	0.0521	0.0752
Ana. N=3	0.0148	0.0237	0.0358	0.0521	0.0752
Asy. N=3	0.0151	0.0241	0.0365	0.0538	0.0784
Greedy N=3	0.0141	0.0219	0.0318	0.0445	0.0613
Sim. N=5	0.0357	0.0668	0.1206	0.2155	0.3769
Ana. N=5	0.0357	0.0668	0.1206	0.2155	0.3769
Asy. N=5	0.0365	0.0692	0.1290	0.2441	0.4778
Greedy N=5	0.0310	0.0532	0.0872	0.1422	0.2316

Table 6 Data for Fig.7

f_{total}/GHz	1	3	5	7	9
Sim. N=3	0.1330	0.0413	0.0358	0.0337	0.0326
Ana. N=3	0.1330	0.0413	0.0358	0.0337	0.0326
Asy. N=3	0.1434	0.0423	0.0365	0.0344	0.0334
Greedy N=3	0.0667	0.0334	0.0318	0.0310	0.0306
Sim. N=5	1	0.1771	0.1206	0.1051	0.0976
Ana. N=5	1	0.1771	0.1206	0.1051	0.0976
Asy. N=5	1	0.1959	0.1290	0.1112	0.1030
Greedy N=5	0.4578	0.1018	0.0872	0.0837	0.0820

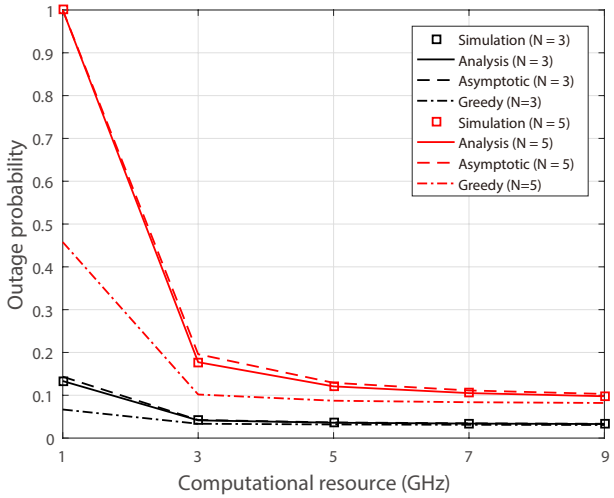

Figure 7. System outage probability versus total computational resource f_{total}.

varies, which illustrates the accuracy of our methods with various computational resources. Moreover, for either $N = 3$ or $N = 5$, the system outage probabilities decrease as the computational resource increases, because a larger computational resource enhances the performance of the system. In further, the system with $N = 5$ has a larger outage probability than that with $N = 3$, since the increase in the number of mobile users exacerbates the competition for limited resources in the system.

6. Conclusions

In this paper, a novel real-time task fault-tolerant scheduling algorithm was presented for a dynamic monitoring platform of distribution network operation. The platform was frequently subjected to overload from distribution transformers. To address this issue, the proposed algorithm utilized wireless communication and mobile edge computing. For the considered system, we evaluated the system performance by analyzing the communication and computing latency, from which we then derived an analytical expression of system outage probability to facilitate the performance evaluation. We further optimized the system design by allocating computing resources for multiple mobile users, where a greedy-based optimization scheme was proposed. Simulations were conducted to demonstrate the effectiveness of the proposed algorithm in reducing task completion time, improving resource utilization, and enhancing system reliability. Overall, this study offered a practical solution for the dynamic monitoring of distribution networks.

6.1. Copyright

7. Acknowledgements

The work in this paper was supported by the Innovation Project of China Southern Power Grid (No. GDKJXM20210995).

References

[1] W. Hong, J. Yin, M. You, H. Wang, J. Cao, J. Li, and M. Liu, "Graph intelligence enhanced bi-channel insider threat detection," in *Network and System Security: 16th International Conference, NSS 2022, Denarau Island, Fiji,*

December 9–12, 2022, Proceedings. Springer, 2022, pp. 86–102.

[2] H. Hui and W. Chen, "Joint scheduling of proactive pushing and on-demand transmission over shared spectrum for profit maximization," *IEEE Trans. Wirel. Commun.*, vol. 22, no. 1, pp. 107–121, 2023.

[3] R. Zhao, C. Fan, J. Ou, D. Fan, J. Ou, and M. Tang, "Impact of direct links on intelligent reflect surface-aided mec networks," *Physical Communication*, vol. 55, p. 101905, 2022.

[4] W. Zhou, L. Fan, F. Zhou, F. Li, X. Lei, W. Xu, and A. Nallanathan, "Priority-aware resource scheduling for UAV-mounted mobile edge computing networks," *IEEE Transactions on Vehicular Technology*, 2023.

[5] J. Yin, M. Tang, J. Cao, M. You, H. Wang, and M. Alazab, "Knowledge-driven cybersecurity intelligence: software vulnerability co-exploitation behaviour discovery," *IEEE Transactions on Industrial Informatics*, 2022.

[6] W. Zhou and F. Zhou, "Profit maximization for cache-enabled vehicular mobile edge computing networks," *IEEE Trans. Vehic. Tech.*, vol. PP, no. 99, pp. 1–6, 2023.

[7] L. F. Abanto-Leon, A. Asadi, A. Garcia-Saavedra, G. H. Sim, and M. Hollick, "Radiorchestra: Proactive management of millimeter-wave self-backhauled small cells via joint optimization of beamforming, user association, rate selection, and admission control," *IEEE Trans. Wirel. Commun.*, vol. 22, no. 1, pp. 153–173, 2023.

[8] J. Yin, M. Tang, J. Cao, H. Wang, M. You, and Y. Lin, "Vulnerability exploitation time prediction: an integrated framework for dynamic imbalanced learning," *World Wide Web*, pp. 1–23, 2022.

[9] S. Tang and L. Chen, "Computational intelligence and deep learning for next-generation edge-enabled industrial IoT," *IEEE Trans. Netw. Sci. Eng.*, vol. 9, no. 3, pp. 105–117, 2022.

[10] Y. Wu and C. Gao, "Intelligent resource allocation scheme for cloud-edge-end framework aided multi-source data stream," *to appear in EURASIP J. Adv. Signal Process.*, vol. 2023, no. 1, 2023.

[11] S. Tang and X. Lei, "Collaborative cache-aided relaying networks: Performance evaluation and system optimization," *IEEE Journal on Selected Areas in Communications*, vol. 41, no. 3, pp. 706–719, 2023.

[12] X. Zheng and C. Gao, "Intelligent computing for WPT-MEC aided multi-source data stream," *to appear in EURASIP J. Adv. Signal Process.*, vol. 2023, no. 1, 2023.

[13] R. Zhang, B. Shim, and W. Wu, "Direction-of-arrival estimation for large antenna arrays with hybrid analog and digital architectures," *IEEE Trans. Signal Process.*, vol. 70, pp. 72–88, 2022.

[14] L. Chen and X. Lei, "Relay-assisted federated edge learning:Performance analysis and system optimization," *IEEE Transactions on Communications*, vol. PP, no. 99, pp. 1–12, 2022.

[15] Z. Na, B. Li, X. Liu, J. Wan, M. Zhang, Y. Liu, and B. Mao, "Uav-based wide-area internet of things: An integrated deployment architecture," *IEEE Netw.*, vol. 35, no. 5, pp. 122–128, 2021.

[16] J. Ling and C. Gao, "DQN based resource allocation for NOMA-MEC aided multi-source data stream," *to appear in EURASIP J. Adv. Signal Process.*, vol. 2023, no. 1, 2023.

[17] S. Mosharafian and J. M. Velni, "Cooperative adaptive cruise control in a mixed-autonomy traffic system: A hybrid stochastic predictive approach incorporating lane change," *IEEE Trans. Veh. Technol.*, vol. 72, no. 1, pp. 136–148, 2023.

[18] R. Zhao and M. Tang, "Profit maximization in cache-aided intelligent computing networks," *Physical Communication*, vol. PP, no. 99, pp. 1–10, 2022.

[19] B. Banerjee, R. C. Elliott, W. A. Krzymien, and H. Farmanbar, "Downlink channel estimation for FDD massive MIMO using conditional generative adversarial networks," *IEEE Trans. Wirel. Commun.*, vol. 22, no. 1, pp. 122–137, 2023.

[20] L. He and X. Tang, "Learning-based MIMO detection with dynamic spatial modulation," *IEEE Transactions on Cognitive Communications and Networking*, vol. PP, no. 99, pp. 1–12, 2023.

[21] H. Wan and A. Nosratinia, "Short-block length polar-coded modulation for the relay channel," *IEEE Trans. Commun.*, vol. 71, no. 1, pp. 26–39, 2023.

[22] L. Zhang and S. Tang, "Scoring aided federated learning on long-tailed data for wireless iomt based healthcare system," *IEEE Journal of Biomedical and Health Informatics*, vol. PP, no. 99, pp. 1–12, 2023.

[23] H. Ma, Y. Fang, P. Chen, S. Mumtaz, and Y. Li, "A novel differential chaos shift keying scheme with multidimensional index modulation," *IEEE Trans. Wirel. Commun.*, vol. 22, no. 1, pp. 237–256, 2023.

[24] Z. Na, Y. Liu, J. Shi, C. Liu, and Z. Gao, "Uav-supported clustered NOMA for 6g-enabled internet of things: Trajectory planning and resource allocation," *IEEE Internet Things J.*, vol. 8, no. 20, pp. 15 041–15 048, 2021.

[25] W. Wu, F. Zhou, R. Q. Hu, and B. Wang, "Energy-efficient resource allocation for secure noma-enabled mobile edge computing networks," *IEEE Trans. Commun.*, vol. 68, no. 1, pp. 493–505, 2020.

[26] W. Wu, F. Zhou, B. Wang, Q. Wu, C. Dong, and R. Q. Hu, "Unmanned aerial vehicle swarm-enabled edge computing: Potentials, promising technologies, and challenges," *IEEE Wirel. Commun.*, vol. 29, no. 4, pp. 78–85, 2022.

[27] W. Zhou, C. Li, and M. Hua, "Worst-case robust MIMO transmission based on subgradient projection," *IEEE Commun. Lett.*, vol. 25, no. 1, pp. 239–243, 2021.

[28] J. Ren, X. Lei, Z. Peng, X. Tang, and O. A. Dobre, "Ris-assisted cooperative NOMA with SWIPT," *IEEE Wireless Communications Letters*, 2023.

[29] W. Xu, Z. Yang, D. W. K. Ng, M. Levorato, Y. C. Eldar, and M. Debbah, "Edge learning for B5G networks with distributed signal processing: Semantic communication, edge computing, and wireless sensing," *IEEE J. Sel. Top. Signal Process.*, vol. 17, no. 1, pp. 9–39, 2023.